**Title:** Enhancing electroporation-induced liposomal drug release in suspension and solid phases

**Authors**: Abby Silbaugh[a]* Joseph Vallin[a]*, Francisco Pelaez[a], Mihee Kim[a], Qi Shao[b], Han Seung Lee[c], John C. Bischof [b,d], Samira M. Azarin[a†]

[a] Department of Chemical Engineering and Materials Science, University of Minnesota, Minneapolis, MN 55455, USA

[b] Department of Mechanical Engineering, University of Minnesota, Minneapolis, MN 55455, USA

[c] Characterization Facility, College of Science and Engineering, University of Minnesota, Minneapolis, MN 55455, USA

[d] Department of Biomedical Engineering, University of Minnesota, Minneapolis, MN 55455, USA

*These authors contributed equally to this work

[†]Address correspondence to Samira M. Azarin (azarin@umn.edu)

**Keywords**: electroporation, liposome, on-demand drug delivery, membrane fluidity, polymer scaffold, thermal stability

**Abstract**: When exposed to an external electric field, lipid bilayer membranes are subject to increased permeability through the generation of pores. Combining this phenomenon, known as electroporation, with liposomal drug delivery offers the added benefit of on-demand release of the liposomal cargo. In previous studies, the maximum percent drug release when exposing liposomes to a pulsed electric field has not surpassed 30%, indicating most of the drug is still retained in the liposomes. Here we showed that by modulating the fluidity of the liposome membrane through appropriate selection of the primary lipid, as well as the addition of other fluidity modulating components such as cholesterol and biotinylated lipid, the electroporation-induced percent release could be increased to over 50%. In addition to improved induced release from liposomes in suspension, biomaterial scaffold-bound liposomes were developed. Electroporation-induced protein release from this solid phase was verified after performing further optimization of the liposome formulation to achieve increased stability at physiological temperatures. Collectively, this work advances the ability to achieve efficient electroporation-induced liposomal drug delivery, which has the potential to be used in concert with other clinical applications of electroporation, such as gene electrotransfer and irreversible electroporation (IRE), in order to synergistically increase treatment efficacy.

## 1. Introduction

Over the past several decades, liposomal drug encapsulation has become a standard for controlled therapeutic delivery and paved the way for more sophisticated forms of nanomedicine. Chief among the benefits of liposomal drug delivery are reduced toxicity (Kedar et al., 1997; Alexander H van der Veen et al., 1998), improved pharmacokinetics (Anderson et al., 1994; Gabizon and Papahadjopoulos, 1988), protection of the cargo from enzymatic degredation (Niu et al., 2011), as well as the ability to modify the carrier surface for decreased detection (Kim et al., 2002) or targeted distribution to specific cells or diseased sites (Belhadj et al., 2017). These attributes have motivated the use of liposomes as protective delivery vehicles for large biological pharmaceuticals. Liposomes or lipid nanoparticles have been successfully utilized as carriers for vaccine antigens (Altin and Parish, 2006; Mulligan et al., 2020; Wassef et al., 1994; Yoshizaki et al., 2014), for oral insulin delivery (Niu et al., 2011; Zhang et al., 2014), and for cytokine immunomodulators used to treat cancer (Kedar et al., 1997; Alexander H. van der Veen et al., 1998) and infectious disease (Mbawuike et al., 1990). Despite these benefits, there is little control over when and how much drug is released from the liposomes after administration. For example, for cell surface receptor targets it would be beneficial to achieve maximal drug release prior to intracellular uptake of the liposomes. To address this shortcoming, several approaches have been explored to obtain an inducible release of liposomal cargo. Yuyama et al. created a thermosensitive liposome platform from which cargo could be released following application of focal hyperthermia after passive liposome accumulation in a murine sarcoma tumor (Yuyama et al., 2000). Similarly, Forbes et al. utilized near-infra-red laser irradiation to induce reversible release of drug from thermosensitive liposomes tethered to hollow gold nanoshells (Forbes et al., 2014). Another approach is to employ electroporation: a simple, nonthermal method to increase the permeability of lipid bilayers through the generation of pores upon exposure to an electric field. Although more

often studied in the context of cells, Teissie and Tsong were the first to experimentally demonstrate that transient, electrically-induced pores could also be formed in the much smaller lipid vesicle (Teissie and Tsong, 1981). Since then, electroporation of vesicles or liposomes has proven useful in gene electrotransfer (Machy et al., 1988), electrofusion (Stoicheva and Hui, 1994; Stromberg et al., 2001), on-demand controlled drug release (Denzi et al., 2017; Kulbacka et al., 2016; Retelj et al., 2013; Srimathveeravalli et al., 2018), and as a method for loading therapeutics into extracellular vesicles (Lamichhane et al., 2015; Pomatto et al., 2019).

The mechanism of electroporation-induced drug release lies in the dielectric breakdown of the electrically insulating phospholipid membrane, resulting in the formation of nanometer-scale aqueous pores (Davalos et al., 2005). The prevailing theory, substantiated by numerous molecular dynamics studies, is that small "fingerlike" hydrophobic pores, which develop naturally due to random thermal fluctuations among the phospholipids, are stabilized and enlarged by the applied electric field (Golberg and Yarmush, 2013; Kotnik et al., 2012). Interaction between the electric field and the intrinsic dipoles of the phospholipids favors the realignment of adjacent phospholipids to form a hydrophilic pore, which reduces the interfacial pore energy (Glaser et al., 1988; Weaver, 1993). By increasing either the magnitude of the electric field or the size of the liposome, a greater proportion of the liposomal surface area is susceptible to this pore formation, making the adjustment of these parameters a common and useful way to increase transmembrane permeability (Rols and Teissié, 1990). Recent literature has also suggested that the composition of the lipid bilayer plays a non-trivial role in this process, as lipid bilayers with increased surface viscosity or bending stiffness require higher electric fields to undergo the same degree of membrane deformation (Karal et al., 2020; Knorr et al., 2010; Perrier et al., 2018). This suggests membrane composition is another suitable parameter by which electroporation-induced drug

release can be modulated. Once formed, electrically induced pores persist on the time scale of milliseconds to tens of seconds and allow for diffusive and, if charged, electrophoretic transport of molecules across the bilayer (Sukharev et al., 1992).

Unfortunately, to date, using electroporation to release the cargo of liposomes is still an inefficient process, with the highest values for percent release reported in literature ranging from 10-30% (Teissie and Tsong, 1981; Yi et al., 2013). Optimization of the percent release in these studies was limited to modulating electroporation parameters such as electric field strength and pulse number as well as adding a pore-stabilizing amphiphilic peptide; investigation into the effects of the liposomal lipid constituents was absent. Additionally, while much research has been conducted on the electroporation of liposomes in suspension, the electroporation of liposomes bound to a solid phase is understudied. A major application for solid-phase liposomes is the design of multi-functional biomaterial scaffolds (Cheung et al., 2018; Feiner et al., 2018; Guo et al., 2019) that employ tethered liposomes as an inducible release system for tissue engineering purposes. Scaffolds are often designed to provide a continuous, sustained release of various drugs or biological factors to act on the surrounding cellular microenvironment, but there is often no way to interface with the scaffold to start or stop the release. Utilizing scaffold-bound liposomes in conjunction with electroporation would allow for this increased temporal and spatial control over cargo release.

This study aims to address both the issue of inefficient electroporation-induced release as well as the lack of research on electroporation-induced release from solid phase liposomes. First, we show that the percent release of electroporated liposomes in suspension can be increased beyond what has been previously demonstrated (Teissie and Tsong, 1981; Yi et al., 2013) by modulating the lipid composition and the concomitant membrane fluidity. Second, we develop and

test a liposome-bearing, microporous poly(caprolactone) (PCL) scaffold to demonstrate electroporation-induced liposomal drug release from a solid phase. We conclude by performing a proof-of-concept electroporation-mediated release of the inflammatory and immunomodulating cytokine, tumor necrosis factor alpha (TNF-α), from the scaffold-bound liposomes, thus validating the potential feasibility and usefulness of electroporation-mediated release of biomolecules from a solid phase.

## 2. Materials and Methods

### *2.1 Materials and Reagents*

The following reagents were used for the current study: poly(caprolactone) (MilliporeSigma, USA; $M_n$ 80,000), dichloromethane (MilliporeSigma, USA), poly(vinyl alcohol) (Polysciences Inc., USA; $M_w$ 25,000, 88% hydrolyzed, reagent grade), sodium chloride (MilliporeSigma, USA), ethanol (Decon Laboratories, Inc., USA; 200 proof), ethylenediamine (MilliporeSigma, USA), isopropyl alcohol (MilliporeSigma, USA), fluorescamine (MilliporeSigma, USA), acetone (MilliporeSigma, USA), 1,2-dipalmitoyl-sn-glycero-3-phosphocholine (DPPC) (Avanti Polar Lipids Inc., USA), 1-palmitoyl-2-oleoyl-glycero-3-phosphocholine (POPC) (Avanti Polar Lipids Inc., USA), 1,2-dipalmitoyl-sn-glycero-3-phosphoethanolamine-N-(biotinyl) (Avanti Polar Lipids Inc., USA), cholesterol (ovine) (Avanti Polar Lipids Inc., USA), chloroform (MilliporeSigma, USA), carboxyfluorescein (MilliporeSigma, USA), 1 M Tris buffer, pH 8 (Thermo Fisher Scientific, USA), polycarbonate membranes (Whatman, USA), 2-(N-morpholino)ethanesulfonic acid (MES) (Thermo Fisher Scientific, USA), streptavidin (MilliporeSigma, USA), 1-ethyl-3-(3-dimethylaminopropyl)carbodiimide hydrochloride (EDC) (Thermo Fisher Scientific, USA), 1M

Tris buffer, pH 7.4 (Genesee Scientific, USA), Triton X-100 (MilliporeSigma, USA), TNF-α (Sino Biological, USA), human TNF-α ELISA kit (Thermo Fisher Scientific, USA).

*2.2 Scaffold fabrication*

Polymer scaffolds were fabricated from PCL microspheres, which were prepared as previously described (Pelaez et al., 2020; Rao et al., 2016). Briefly, PCL microspheres were generated by emulsifying a 6% (w/w) solution of PCL in dichloromethane with a 10% (w/w) poly(vinyl alcohol) solution and homogenizing at 10,000 rpm for 1 min. Microspheres were lyophilized with a FreeZone 2.5 L Freeze Dryer (Labconco, USA) for 48 h at -80 ºC and then mixed with sieved sodium chloride particles (250-425 μm) in a 1:30 (w/w) ratio. Microsphere/sodium chloride mixtures were pressed to 3,300 lbs (15 kN) for 45 s in a 5 mm steel die (Specac, UK). Pressed disks were heated on each side to 60 ºC for 5 min and then foamed at 55.2 bar for approximately 24 h, after which the gas was released at $1.38 \times 10^{-4}$ $m^3 \cdot s^{-1}$. Salt particles were dissolved by submerging disks in deionized (DI) water for 90 min on a rocking platform. The resulting polymer scaffolds were approximately 5 mm in diameter and 2 mm thick. Polymer scaffolds were sterilized by soaking in 70% ethanol and then rinsed with sterile water and dried on a sterile gauze pad. Scaffolds were stored at -80 ºC until further use.

*2.3 Aminolysis of polymer scaffolds*

The aminolysis reaction with PCL scaffolds was adapted from Nisbet et al. (Nisbet et al., 2008). PCL scaffolds were placed in a 0.05 M ethylenediamine solution in isopropyl alcohol and incubated at ambient pressure at either room temperature for 10 min or at 37 ºC for 24 h. Scaffolds

were then rinsed three times with DI water, with a 5 min soak in DI water between each rinse followed by a final 1 h soak prior to use.

*2.4 Primary amine characterization*

Primary amine functionalization of PCL scaffolds was characterized by fluorescence labeling using fluorescamine. PCL scaffolds were placed in a 10 mM fluorescamine solution in acetone. Immediately afterwards, an equal volume of borate buffer, pH 9, was added to the fluorescamine solution. After 10 min, scaffolds were rinsed three times with water, with a 5 min soak between each rinse. Scaffolds were imaged using an EVOS FL Auto Microscope (Thermo Fisher Scientific, USA) equipped with a 357 nm/447 nm excitation/emission wavelength light filter.

*2.5 Liposome formation*

Liposomes were prepared by hydration of lipid films followed by extrusion. Briefly, either DPPC or POPC was combined with biotin-labeled phospholipid and cholesterol in chloroform to form a 13.3 mM total lipid solution. 4 μmol of total lipid, dissolved in 300 μL chloroform, was placed in a 5 mL round bottom flask and heated to 50 ºC, then dried using a rotatory evaporator (LabTech Srl, Italy) at 60 rpm under vacuum for 5 min to form a thin lipid film. The films were lyophilized overnight at -80 ºC. Each film was then hydrated with 500 μL of 90 mM carboxyfluorescein in an internal buffer comprised of 1 M Tris buffer, pH 8, with varying concentrations of NaCl for 3 h at 50 ºC in a water bath with periodic gentle agitation. Hydrated lipids were then extruded through a 100 nm, 200 nm, 1 μm, or 10 μm polycarbonate membrane 27 times using a manual extruder (Avanti Polar Lipids Inc., USA) at 50 ºC or room temperature for

DPPC or POPC liposomes, respectively. Liposomes were separated from the unencapsulated solution using a PD MiniTrap G-25 Sephadex column (GE Healthcare, USA) flushed with 1 mL of an external buffer comprised of 1 M Tris buffer, pH 8 or 7.4, with varying concentrations of NaCl. Approximately 500-600 μL of liposomal solution was collected, the volume at which the front of the free carboxyfluorescein had reached the bottom of the column. Liposome solutions were either used immediately or stored at 4 ºC prior to use. Liposome size was characterized by dynamic light scattering using a Nanotrac Flex particle size analyzer (Microtrac, USA).

*2.6 Modification of scaffolds with tethered liposomes*

Aminolyzed scaffolds were functionalized with streptavidin by soaking them for 2 h at room temperature in an MES conjugation buffer (0.1 M MES, 0.9% NaCl, pH 4.7) containing 60 nM streptavidin and 6.5 mM EDC. Following conjugation, the scaffolds were washed with 3 rounds of DI water and then soaked in DI water for 1 h. Streptavidin-conjugated scaffolds were then stored in DI water at 4 ºC or immediately loaded with liposomes. To tether the liposomes to the scaffold surface, streptavidin-conjugated scaffolds were partially dried, immersed in liposome solution (~300 μL/scaffold), and incubated at 4 ºC on a rocker overnight (>12 h). Non-bound liposomes were removed by washing the scaffolds at least 3 times using 1M Tris buffer, pH 7.4, and then soaking them in buffer for 1 h. Liposome-tethered scaffolds were used immediately for experimentation.

*2.7 Electroporation treatment and dye release measurement*

A volume of 130 μL of each prepared liposome solution was placed in an electroporation cuvette with aluminum plate electrodes spaced 2 mm apart (Fisher Scientific, USA). The two

electrodes were then connected to an ECM 830 electrical pulse generator (BTX/Harvard Apparatus, USA) in order to induce a homogeneous electric field throughout the liposome solution. The electric field was determined by dividing the applied voltage by the distance between the electrodes. Liposomes were subjected to either 500, 1500, or 2000 $V \cdot cm^{-1}$ in 99 square pulses with 100 μs pulse duration at a frequency of 1 Hz. Release of encapsulated carboxyfluorescein following electroporation was determined from the fluorescence intensity of the solution. 100 μL of treated liposome solution was placed in a well of a black, round-bottom 96-well plate (Corning, USA) and fluorescence intensity (490 nm/520 nm excitation/emission wavelength) was quantified with a Synergy H1 microplate reader (BioTek Instruments Inc., USA). For positive controls representing total release, liposomes were mixed in equal volume with 2-4% Triton X-100 to disrupt liposome assembly. Untreated liposomal solution was used as a negative control. Percent Release (%), was calculated using the following formula:

$$Percent\ Release\ (\%) = 100 * \frac{F_S - F_-}{2 * F_+ - F_-} \quad (1)$$

where $F_s$, $F_-$, and $F_+$, are the fluorescent intensities of the treated sample, negative control, and positive control, respectively. The fluorescent intensity of the positive control, $F_+$, is multiplied by a factor of 2 to account for the 1:1 dilution with Triton X-100.

*2.8 Liposomal stability assessment*

Carboxyfluorescein-loaded liposomes, either in free solution or tethered to scaffolds, were fabricated as mentioned above and incubated at either 4 ºC or 37 ºC in external buffer (pH 7.4, 1 M Tris buffer, 150 mM NaCl). At days 0 (i.e. no incubation), 2, and 4, aliquots were removed, electroporated, and analyzed with a microplate reader to measure the fluorescence. Liposome-tethered scaffolds were treated with electroporation in a similar manner as the liposomal solution

by placing the scaffolds in an electroporation cuvette filled with 130 μL of external buffer. Stability was quantified as the amount of dye released on day $j$ as a percent of the total release from liposomes electroporated without incubation on day 0 (Normalized Releasable Cargo):

$$Normalized\ Releasable\ Cargo\ (\%) = \frac{F_{s,j} - F_{n,j}}{F_{s,0} - F_{n,0}} * 100 \quad (2)$$

Where $F_{s,j}$ and $F_{n,j}$ are the fluorescence intensities of the electroporated sample and its negative control (not electroporated) after incubation for $j$ days, and $F_{s,0}$ and $F_{n,0}$ are the fluorescence intensities of the electroporated sample and its negative control on day 0. For the stability of liposomes in solution, the negative control, $F_{n,j}$, represents the fluorescence of liposomal solution not treated with electroporation. For the stability of scaffold-bound liposomes, $F_{n,j}$ is calculated as the average fluorescence of untreated scaffold-bound liposomes plus the average fluorescence of electroporation-treated, unmodified PCL scaffolds incubated with liposomes (to account for the effect of non-specific liposome binding).

*2.9 Cryogenic Scanning Electron Microscopy (Cryo-SEM) imaging*

A small portion (approximately 1 μL) of the scaffold specimen was applied to a brass freezer planchet and sandwiched with a second brass freezer planchet. The freezer planchet was scored initially to increase mechanical adhesion between the specimen and the planchet. The HPM010 high pressure freezing machine (Bal-Tec AG, Liechtenstein) was used to freeze the sample. The cooling time from room temperature to -182 °C was achieved within 5-8 ms at 2,100 bar. The frozen sample was mounted onto a specimen holder in a cryo-preparation workstation (Leica Mikrosysteme GmbH, Austria) and was transferred into an EM ACE600 high vacuum sputter coater (Leica Mikrosysteme GmbH, Austria) via an EM VCT100 shuttle (Leica Mikrosysteme GmbH, Austria). The specimen stayed in the specimen holder pre-cooled with

liquid nitrogen during the transfer. The specimen was cleaved with a pre-cooled knife manually at -153 °C. After cleavage, the fractured specimen was heated to -105 °C at a rate of 3 °C per min and sublimed for 10 min. After the sublimation, the fractured specimen was sputter coated with platinum at around -116 °C, giving a thickness of 5 nm. The specimen was imaged at -112 °C with 1 kV accelerating voltage using the SU8230 CFE-SEM (Hitachi High Technologies, Japan).

*2.10 Liposomal TNF-α release*

To produce liposomes loaded with TNF-α, lipid films with a composition of 80:10:10 DPPC:cholesterol:biotinylated lipid were prepared as described above. The films were hydrated for 3 h at 50 ºC with 300 μL of an internal buffer consisting of 1M Tris buffer at pH 8 and either 200 mM or 300 mM NaCl. Liposomes were extruded through a 200 nm polycarbonate membrane as described above and then mixed with a solution of human TNF-α reconstituted in the same hydration buffer as the liposomes such that a final TNF-α concentration of 800 μg/mL was obtained. To encapsulate the TNF-α, two freeze-thaw cycles were performed, as recommended by Costa et al., by placing the liposome suspension in liquid nitrogen for 20 s followed by a passive thaw at room temperature (Costa et al., 2014). TNF-α loaded liposomes were separated from non-encapsulated TNF-α by 2 cycles of ultracentrifugation for 30 min at 70,000 g using an Avanti J-20 XP centrifuge (Beckman Coulter, USA). The liposomes were resuspended in the internal buffer and incubated with streptavidin-conjugated scaffolds as previously described for carboxyfluorescein-loaded liposomes (approximately 300 μL liposomal solution/scaffold). The liposome-tethered scaffolds were then washed 2 times and soaked for 75 min using the matching internal buffer and finally washed once more using an external buffer of 1 M Tris at pH 7.4 with 150 mM NaCl. The scaffolds were then incubated in external buffer at 37 ºC for 0, 2, or 4 days

before being treated with electroporation as described above. The treated solutions were centrifuged at 500 g for 5 min to remove PCL scaffold debris and then frozen and stored at -80 ºC. The presence of TNF-α in the release solution was measured using ELISA with a slight modification of the manufacturer's instruction: wells for samples were loaded with 50 μL of the external buffer from liposome preparation instead of the provided incubation buffer. The amount of electroporation-induced liposomal TNF-α released was calculated as the concentration of TNF-α in the release solution of the streptavidin-conjugated scaffolds minus the average concentration of TNF-α in the release solution of 4 unmodified, plain PCL scaffolds.

### *2.11 Statistical analysis*

Data are the result of three or more biological replicates and are presented as mean ± standard deviation (SD) or standard error of the mean (SEM), as indicated in the figure captions. Statistical significance was determined using GraphPad Prism software with one- or two-way ANOVA as appropriate, and *p*-values were calculated using Tukey's method for multiple comparisons, with $p < 0.05$ considered significant. For the design of experiment study performed in section 3.4, a Box-Behnken statistical design with 12 edge points and 4 center points was used. The resulting data were fit to a second order model using the response-surface regression (rsm) function in R statistical software. Significance of each factor was assessed using ANOVA with Type III contrasts to account for unbalanced data.

## 3. Results

### *3.1 Fabrication of scaffold-bound liposomes*

The process for fabricating the scaffold-bound liposomes is depicted in Scheme 1. Microporous PCL scaffolds were chosen as the solid phase backbone for liposomal tethering, as they are known to facilitate cellular integration (Azarin et al., 2015; Rao et al., 2016), and we have previous experience utilizing them for tissue engineering purposes (Lam et al., 2020; Pelaez et al., 2018) including modifying them with metal mesh electrodes to allow for uniform irreversible electroporation (IRE) of the infiltrated tissue within the scaffold (Pelaez et al., 2020). We hypothesized that liposomes could be securely bound to the scaffold surface using a streptavidin-biotin connection, with streptavidin conjugated to the polymer surface and biotin to a fraction of the liposomal lipids. We first activated the PCL scaffold surface with an aminolysis reaction to allow for further surface modification. This introduced primary amine functionality by partially degrading the PCL ester linkages. To validate sufficient transformation of the surface chemistry, we labeled the scaffold primary amine groups with fluorescamine and measured the resulting fluorescence. An aminolysis reaction occurring at 37 ºC for 24 h generated the highest yield of primary amine groups (Fig. 1A-E), so these parameters were chosen to modify all subsequent scaffolds. Following the introduction of primary amines, the scaffolds were subjected to a carbodiimide coupling reaction to conjugate streptavidin to the scaffold surface. Next, phosphatidylcholine-based liposomes were generated using up to 20% biotinylated lipid (BL) and varying amounts of cholesterol and then incubated with the scaffolds overnight to allow for binding.

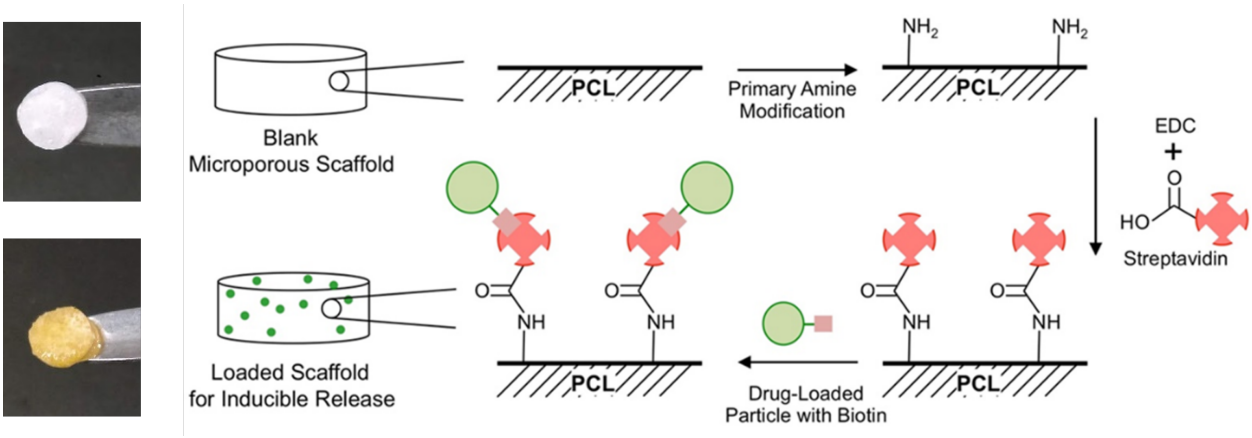


**Scheme 1.** Schematic for attaching drug-loaded liposomes onto microporous polymer scaffolds. PCL scaffolds were chemically modified with primary amines. EDC was used to catalyze the covalent bond between the carboxyl groups on streptavidin and primary amines on modified PCL scaffolds. The strong streptavidin-biotin interaction facilitated the binding of drug-loaded particles (green sphere) labeled with biotin (pink square) to PCL scaffolds for inducible release.

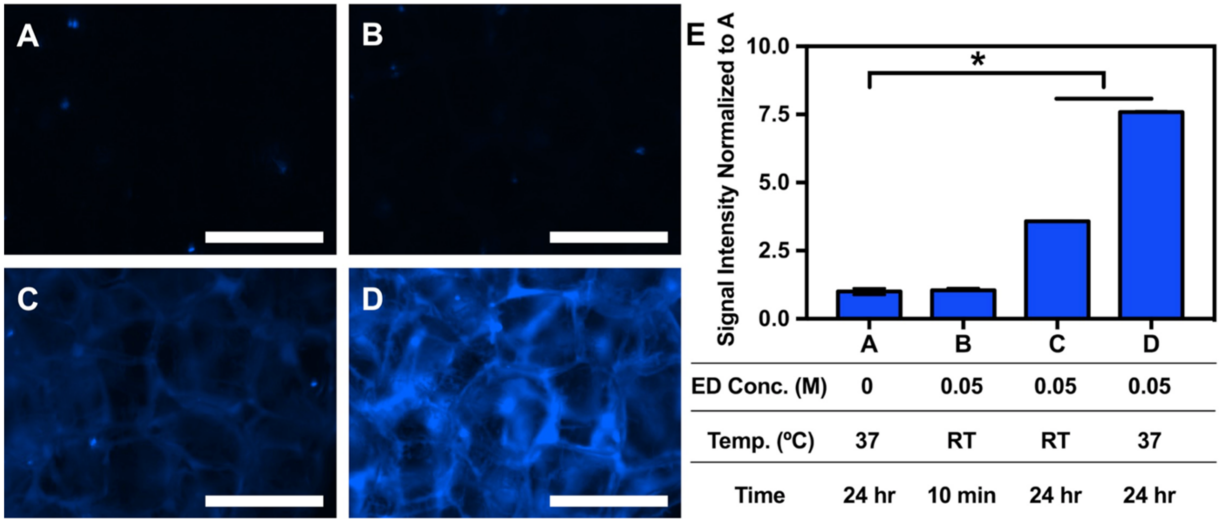


**Fig. 1.** Evaluation of PCL scaffold surface activation with primary amines. (A-D) Fluorescence imaging of microporous PCL scaffolds after no ethylenediamine (ED) reaction (A) or 0.05 M ethylenediamine in isopropyl alcohol at room temperature (RT) for 10 min (B) or 24 h (C), or at 37 ºC for 24 h (D). All scaffolds were treated with fluorescamine to fluorescently label primary amines. Scale bar indicates 500 μm. (E) Average signal intensity taken from scaffold samples normalized to scaffolds treated without ethylenediamine. Intensity values were averaged over the three individual scaffold samples per reaction condition. The average intensity per scaffold was quantified from four separate images taken for each scaffold. * $p < 0.001$ compared to scaffolds treated without ethylenediamine. Normalized signal intensity data is mean ± SD, n = 3.

To verify successful tethering of the liposomes to the scaffold following overnight incubation, we examined the surface of the scaffolds using cryo-SEM (Fig. 2). Fig. 2D suggests successful liposome binding, as numerous spheroidal features with an average diameter of 180 ± 40 nm can be seen, which are not observed on the plain PCL scaffold control (Fig. 2C). The size range of these features matches well with the nominally sized 200 nm liposomes that were extruded and used in the fabrication process.

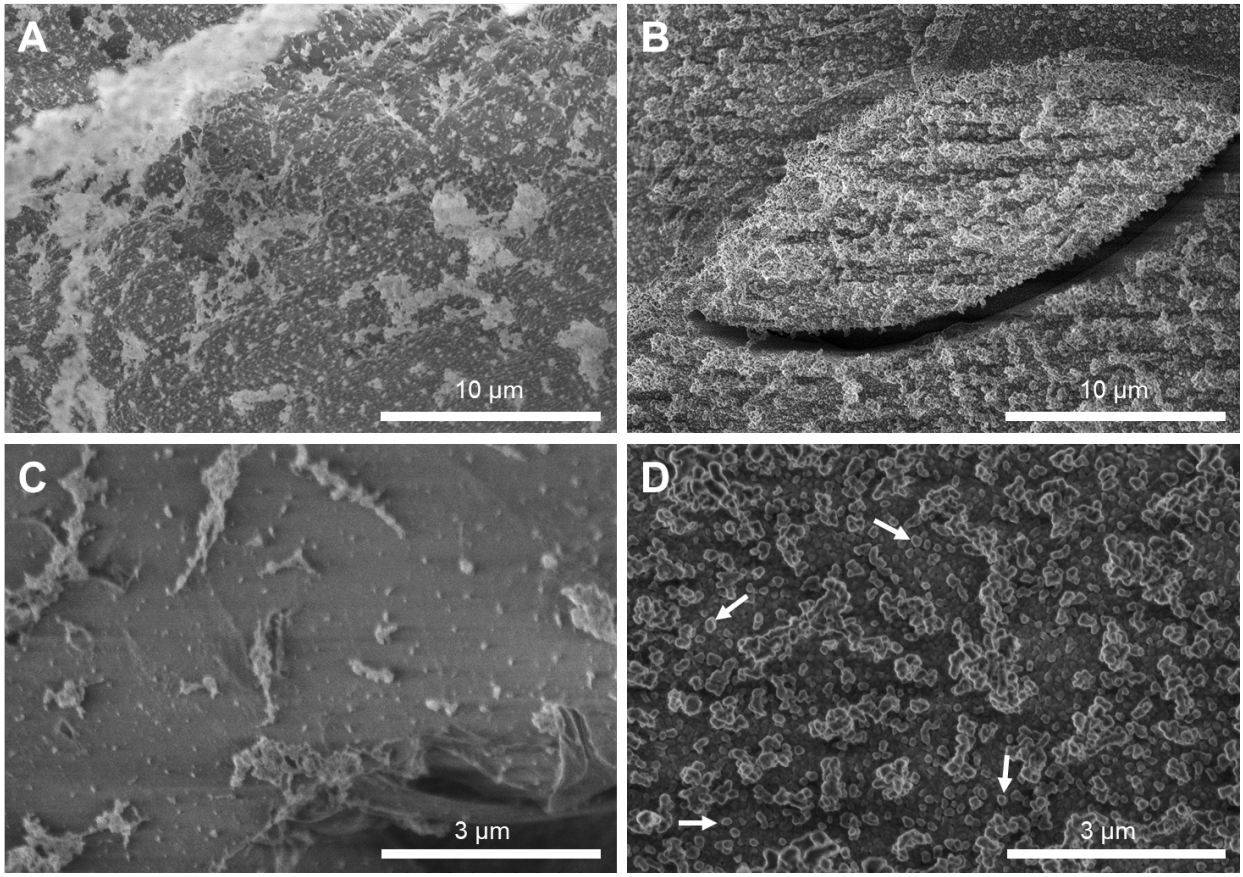


**Fig. 2.** Verification of liposomal attachment to scaffold surface. Representative cryo-SEM images of the scaffold surface for (A, C) a blank PCL scaffold control or (B, D) a liposome-conjugated scaffold bearing nominally 200 nm liposomes with a composition of 80% DPPC/10% cholesterol/10% BL. Round features on (D), a few of which are denoted by white arrows, are 180 ± 40 nm according to ImageJ analysis.

*3.2 Optimizing liposomal parameters for maximal electroporation-induced drug release*

In previous studies exploring electroporation-induced release of a drug from liposomes, only a minimal percent release of the encapsulated cargo was observed (~10-30%) (Teissie and

Tsong, 1981; Yi et al., 2013). Aiming to significantly increase the percent release, we investigated two separate liposome characteristics - formulation and size - for their effect on electroporation-induced release. Two different primary constituent lipids were chosen such that the liposomal membrane would exist at two different phases at physiological temperatures: DPPC to produce an ordered gel phase membrane, and POPC to give a liquid crystalline phase membrane. Liposomes of varying size (Fig. S1) and lipid constituents were electroporated with increasing electric field strengths, and the percent release of an encapsulated, self-quenching fluorescent dye, carboxyfluorescein (CF), was measured (Fig. 3A-C). The percent release increased with size and electric field strength for the DPPC liposomes, as expected. For example, a 2000 $V \cdot cm^{-1}$ electric field achieved a 3.8 ± 0.8% percent release for 100 nm extruded liposomes (Fig. 3A), a 13 ± 2% percent release for 1 μm extruded liposomes (Fig. 3B), and 22 ± 6% percent release for 10 μm extruded liposomes (Fig. 3C). However, these relationships were not seen in the case of POPC liposomes, which released less than 5% of CF over the entire range of both factors. Although percent release increases as liposome size is increased, it has been shown that liposomes with nominal sizes above 200 nm are more likely to be discovered and cleared *in vivo* by phagocytes from the mononuclear phagocyte system (Chu et al., 2016; Alexander H van der Veen et al., 1998). Therefore, we decided to choose a liposome size of 200 nm, the largest possible size subject to this constraint, for all future experiments.

As the percent release for the tested liposomes closest in size to 200 nm (100 nm, Fig. 3A) was still no higher than 5%, we hypothesized that the addition of cholesterol, a modulator of membrane fluidity (Bhattacharya and Haldar, 2000), could increase electroporation-induced CF release from 200 nm liposomes. As seen in Fig. 3D and E, for a low electric field strength (500 $V \cdot cm^{-1}$) an increase in the cholesterol content from 0% to 70% caused a small increase in the

percent release of CF for DPPC (from 0.06 ± 0.05% to 0.9 ± 0.1%) as well as POPC liposomes (from 0.11 ± 0.02% to 1.4 ± 0.4%). However, at high electric field strengths (2000 V·cm$^{-1}$), DPPC liposomes exhibited a decrease in the percent release from 17 ± 3 % to 2 ± 2% as cholesterol content increased from 0% to 70%, but POPC liposomes displayed an increase in percent release from 1.4 ± 0.4% to 6.5 ± 0.2% over the same range. Notably, percent release values for POPC liposomes were consistently smaller than that of the DPPC formulations. Given that percent release was the highest in DPPC liposomes with 0-30% cholesterol under 2000 V·cm$^{-1}$, we decided to focus on optimizing these liposomes in a more localized parameter space. Upon a closer examination of the effects of low cholesterol levels on DPPC liposomes electroporated at 2000 V·cm$^{-1}$ (Fig. 3F), a local maximum in percent release of 25 ± 4% at 20% cholesterol was observed.

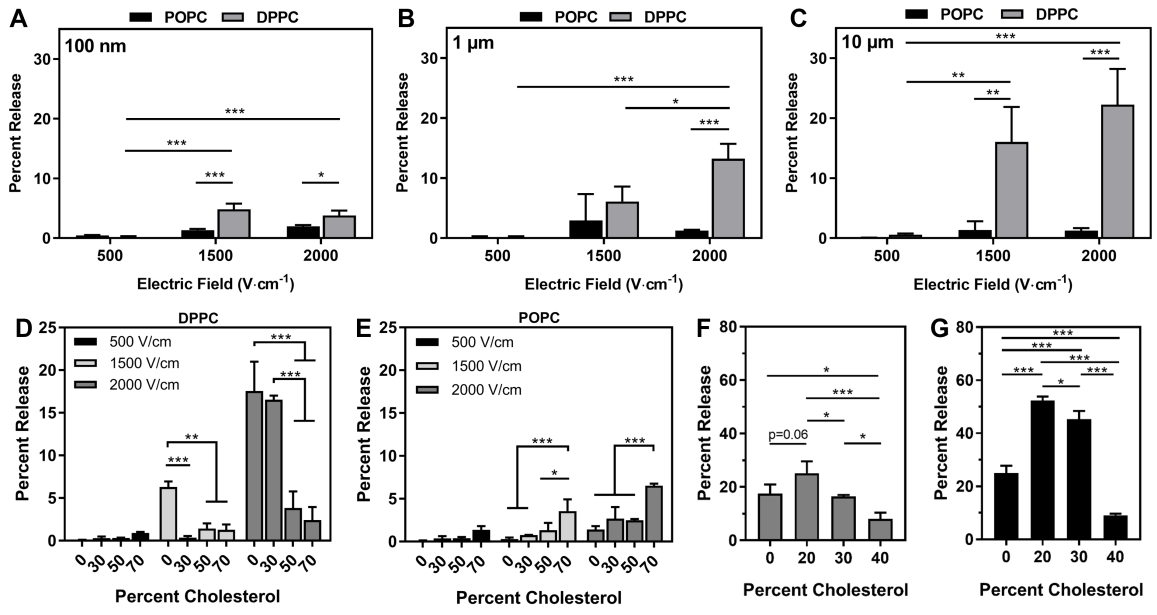


**Fig. 3.** Effect of liposome composition on electroporation-induced release of CF. (A-C) Percent release of CF from POPC and DPPC liposomes following electroporation with 99 pulses at 100 µs pulse duration at 1 Hz at either 500, 1500, or 2000 V·cm$^{-1}$ on liposome preparations extruded though 100 nm (A), 1 µm (B), and 10 µm (C) filters. (D-G) Percent release of CF from 200 nm liposomes with 200 mM NaCl and dispersed in an external buffer of 1 M Tris HCl pH 8. Release was induced by electroporation with 99 pulses at 100 µs pulse duration at 1 Hz. (D-E) Percent release from liposomes with either 500, 1500, or 2000 V·cm$^{-1}$ electric field. Lipid films were composed of either DPPC (D) or POPC (E) with increasing amounts of cholesterol comprising the remainder. (F) Percent release from DPPC liposomes with increasing

amounts of cholesterol at 2000 $V \cdot cm^{-1}$. (G) Percent release from DPPC liposomes with fixed 10% BL and increasing amounts of cholesterol at 2000 $V \cdot cm^{-1}$. (A-G) Percent release is mean ± SD, n = 3. Data was analyzed by two-way (A-E) or one-way (F,G) ANOVA, and multiple comparisons were performed with Tukey's method; * $p < 0.05$, ** $p < 0.01$, *** $p < 0.001$.

Next, we explored the effect of adding BL to the low cholesterol DPPC liposomes, as BL is necessary for the eventual tethering of the liposomes to the PCL scaffold surface. Surprisingly, after the addition of 10% BL to low cholesterol DPPC liposomes, the percent release increased dramatically, but only for DPPC liposomes with 20% and 30% cholesterol, which displayed a two- and three-fold increase in percent release, respectively (Fig. 3G). This suggests a synergistic effect between cholesterol and BL for this range of cholesterol, indicating a promising parameter space for further optimization. Choosing the 20% cholesterol DPPC liposomes, we more thoroughly explored the influence of varying levels of BL. As seen in Fig. 4A, even small amounts of BL (0.1%) caused a large increase in the percent release from 25 ± 4% (0% BL) to 49 ± 1%. However, further increasing the content of BL to 20% only raised the percent release to 56 ± 1%. Finally, we repeated this experiment with the scaffold-bound liposomes rather than liposomes freely suspended in solution (Fig. 4B). Again, higher levels of BL resulted in greater amounts of released CF. These analyses indicate that 20% cholesterol DPPC liposomes with 20% BL (60:20:20 DPPC:cholesterol:BL liposomes) provide maximal electroporation-induced cargo release. Outside of liposomal composition, other minor parameters such as transmembrane gradients in ionic species theoretically have the potential to affect release, however when we varied the internal NaCl concentration (Fig. S2) and the pH of the external buffer (Fig. S3) we observed negligible impacts on percent release for 200 nm liposomes.

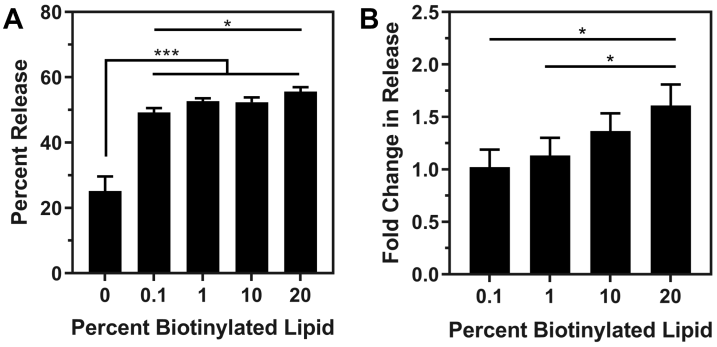


**Fig. 4.** The presence of BL in liposomes significantly increases electroporation-induced CF release. (A) Percent release of CF from 200 nm 20% cholesterol DPPC liposomes containing increasing levels of BL (with an internal concentration of 200 mM NaCl) following electroporation. (B) Fold change in CF release from scaffold-conjugated liposomes with increasing levels of BL compared to those without BL. Liposomes attached to scaffolds were 200 nm DPPC liposomes with 20% cholesterol. They contained 150 mM NaCl and were dispersed in 1 M Tris HCl pH 7.4 with 200 mM NaCl. Fold change in release from scaffolds was determined by normalizing the released fluorescence to that of scaffolds with 80% DPPC/20% cholesterol/0% BL liposomes. Released fluorescence was determined by subtracting the fluorescence of an untreated scaffold control from the fluorescence of the electroporation-treated scaffold with the same liposomal formulation. (A-B) Freely suspended and scaffold-conjugated liposomes were electroporated at 2000 $V \cdot cm^{-1}$ for 99 pulses at 100 μs pulse duration at 1 Hz. Bars are mean ± SD. Results were analyzed with a one-way ANOVA and Tukey's method for multiple comparisons. * $p < 0.05$, ** $p < 0.01$ *** $p < 0.001$.

*3.3 Optimizing membrane composition for liposomal stability at physiological temperatures*

As an on-demand drug delivery system, it is important not only to maximize liposomal drug release upon application of the electrical pulses but also to minimize premature release or leakage of the drug before electroporation is administered. Because the 60:20:20 liposome formulation was shown in our studies to exhibit the highest electroporation-induced drug release, we next assessed its ability to maintain stable barrier properties under exposure to physiological temperature (37 ºC). 60:20:20 liposomes were loaded with CF, and their electroporation-induced release was measured after up to 4 days of incubation in isothermal conditions. As seen in Fig. 5A, although these liposomes retained stability at 4 ºC (typical storage conditions) their barrier

properties diminished extensively when incubated at 37 ºC, with evidence of almost complete leakage by 2 days.

Because of cholesterol's influence on membrane permeability (Briuglia et al., 2015), we varied the cholesterol content between 10% and 30% to examine its effect on preserving the thermal stability of the liposomes. Changing the cholesterol content in this manner did not significantly change the initial (day 0) percent release of CF compared to the original 60:20:20 formulation. Values were maintained between 55 and 58 percent for all conditions (Fig. S4). As seen in Fig. 5B, in the case of the 80:10:10 liposomes, a lower cholesterol content was able to recover membrane stability, and the liposomes still maintained 40 ± 33 % of releasable CF cargo at day 4. In contrast, formulations with higher levels of cholesterol had lost all CF cargo even by day 2. Next, we investigated if the BL content could be increased while still maintaining the stability seen in a liposomal composition with 10% cholesterol, as this might improve liposomal binding to the scaffold. However, increasing the BL content to 20% (with a 70:10:20 liposome formulation) eliminated the thermal stability seen in the 80:10:10 liposomes (Fig. S5). Finally, we sought to validate the improved stability of 80:10:10 liposomes compared to 60:20:20 liposomes when in the scaffold-bound solid phase. Once again, 80:10:10 scaffold-bound liposomes displayed increased stability over 60:20:20 scaffold-bound liposomes (Fig. 5C).

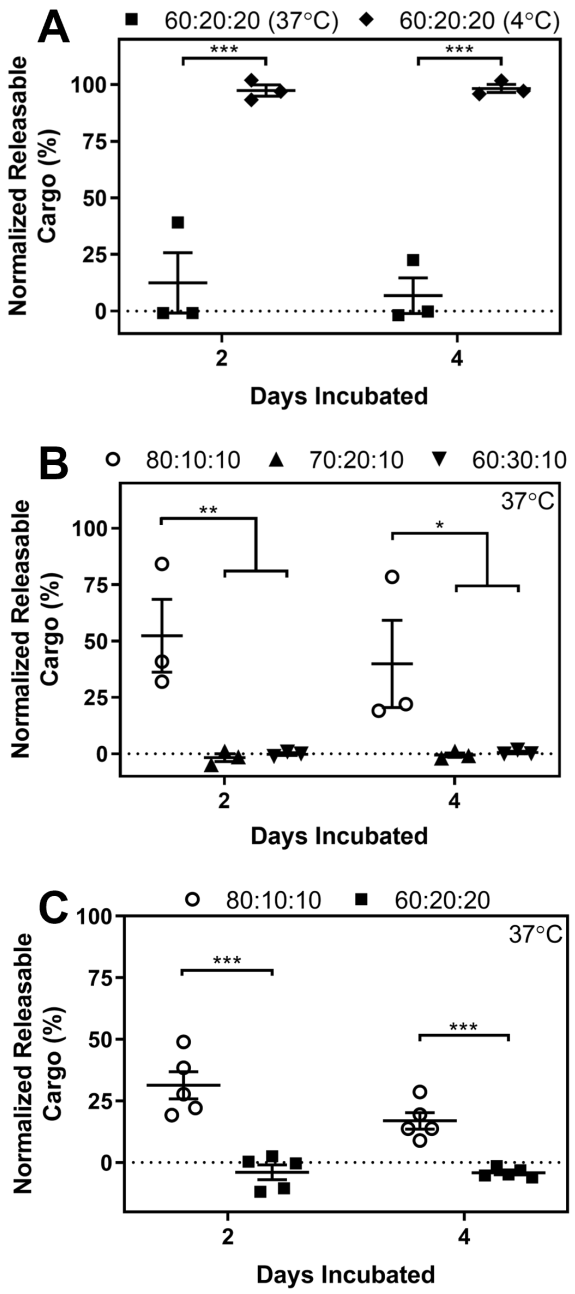


**Fig. 5.** Thermal stability of liposomes and scaffold-bound liposomes at physiological temperature. (A) The percent release of 60% DPPC/20% cholesterol/20% BL liposomes was measured in response to electroporation treatment after 2 and 4 days of pre-incubation at 4 ºC or 37 ºC. Results were normalized to treated liposomes with 0 days of incubation to obtain Normalized Releasable Cargo. (B) Normalized Releasable Cargo for liposomes with varying levels of cholesterol were measured for 2 and 4 days of pre-incubation at 37 ºC. Formulations are described as DPPC:cholesterol:BL. (A-B) Normalized Releasable Cargo is mean ± SEM, n = 3 (C) Normalized Releasable Cargo of scaffold-bound liposomes bearing 200 nm liposomes of either 60% DPPC/20% cholesterol/20% BL or 80% DPPC/10% cholesterol/10% BL after 2 or 4 days of pre-incubation at 37 ºC. Normalized Releasable Cargo is mean ± SEM, n = 5. (A-C) Liposomes, either free or conjugated to a scaffold, contained an internal buffer of 1 M Tris HCl, pH 8, 200

mM NaCl, and were dispersed in an external buffer of 1M Tris HCl, pH 7.4, 150 mM NaCl. All were treated with 99 pulses at 100 μs pulse duration at 1 Hz with an electric field strength of 2000 $V \cdot cm^{-1}$. Data was analyzed with a two-way ANOVA, and multiple comparisons were performed using Tukey's method; * $p < 0.05$, ** $p < 0.01$, *** $p < 0.001$.

Despite the improved stability of the 80:10:10 scaffold-bound liposomes, there was still significant leakage of CF, as over 75% of releasable CF was lost after 4 days of incubation at 37 ºC. Although further decreasing the cholesterol content would likely improve membrane stability, some level of cholesterol is still necessary to allow for an appreciable release upon electroporation (Fig. 3G). However, as the final design goal is the release of a macromolecular cell-signaling cue, which should exhibit a higher retention level given its large size relative to CF, we moved forward with the 80:10:10 formulation for studying electroporation-induced cytokine release.

*3.4 Electroporation-induced release of a macromolecule from scaffold-bound liposomes*

Finally, we inquired if scaffold-bound liposomes could be utilized for electroporation-mediated inducible release of the macromolecule cytokine TNF-α. Acknowledging the larger structure of a protein adjuvant versus the small indicator molecule CF, we allowed for the possibility of a decrease in release due to steric effects and explored the parameter space of several key factors to further increase its induced release from the liposomes. A Box-Behnken statistical design of experiment was performed on TNF-α loaded 80:10:10 liposomes to investigate the effects of the number of electrical pulses applied to the liposomes, the concentration of TNF-α used to load the liposomes, and the initial transmembrane ionic strength difference. By fitting the results to a second order response surface model, we observed that the latter two factors significantly affected the amount of electroporation-induced release (Fig. S6). Accordingly, we assembled TNF-α loaded liposomes with a high loading concentration of TNF-α (800 μg/mL) and a high internal ionic strength (200 and 300 mM NaCl; as compared to 150 mM external NaCl),

and we tethered them to scaffolds. The amount of TNF-α released via electroporation was measured after varying lengths of pre-incubation at 37 ºC. As seen in Fig. 6, scaffold-bound 80:10:10 liposomes successfully released encapsulated TNF-α when subjected to electroporation. Although there was no statistically significant difference in release observed between pairwise comparisons of 0, 2, or 4 days of 37 ºC pre-incubation, the factor of incubation time, as a whole, had a statistically significant effect on the amount of TNF-α released ($p < 0.05$); longer incubation times caused a decrease in the releasable cargo. After 4 days of pre-incubation at 37 ºC, the scaffold-bound liposomes only released 20-50% of the amount of TNF-α that they released with no pre-incubation at 37 ºC. This indicates that cargo leakage is likely still occurring, but not to the same degree as was seen for CF-encapsulating scaffold-bound liposomes.

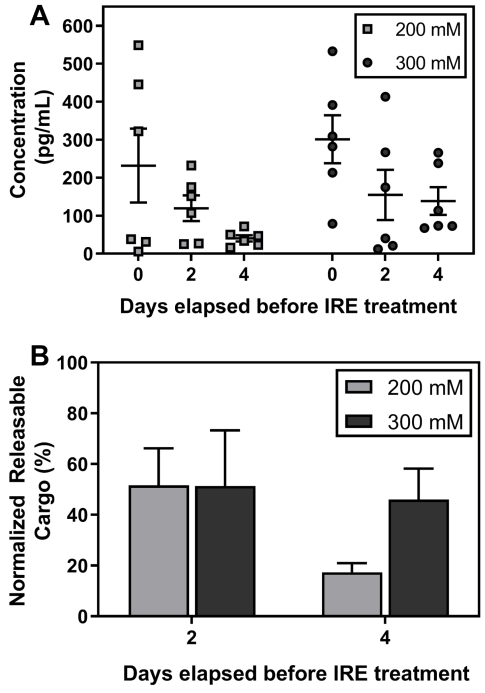


**Fig. 6.** Electroporation-induced release of TNF-α from scaffold-bound liposomes. Scaffold-bound liposomes were fabricated using 200 nm 80% DPPC/10% cholesterol/10% BL liposomes. The liposomes encapsulated TNFα dissolved in 1 M Tris HCl pH 8 with either 300 mM or 200 mM NaCl. The scaffold-bound liposomes were pre-incubated for 0, 2, or 4 days at 37 ºC before being electroporated with 99 pulses with a 100 μs pulse duration at 1 Hz and 2000 $V \cdot cm^{-1}$. The concentration of released TNF-α was measured

(A) and used to calculate the Normalized Releasable Cargo (B). Graphs depict mean ± SEM. Data were analyzed with a two-way ANOVA, which revealed that the factor of time had a statistically significant effect ($p < 0.05$). However, Tukey's method for multiple comparisons revealed no significant difference between any pairwise combination of treatment groups ($p > 0.05$).

## 4. Discussion

In designing an electroporation-triggered drug release system, it is desirable to engender maximal if not complete release of liposomal contents upon application of the pulsating electric field. This can be accomplished by optimizing the factors relating to the mechanism of pore formation and persistence. The central parameter controlling the onset of pore formation is the induced transmembrane voltage, $\Delta\Psi_m$. According to the Schwan equation (3), $\Delta\Psi_m$ is dependent on

$$\Delta\Psi_m = \frac{3}{2} E \cdot R \cdot \cos\theta \left[1 - e^{\frac{-t}{\tau_m}}\right] \quad (3)$$

the magnitude of the electric field, $E$; the radius of the liposome, $R$; the position along the membrane with respect to the direction of the field, $\theta$; time, $t$; and a membrane charging time constant, $\tau_m$, which is a function of membrane properties and the conductivity of the surrounding media (Kotnik et al., 2012). When $\Delta\Psi_m$ modestly surpasses the dielectric strength of the phospholipid bilayer, pore formation is induced in a manner known as *reversible electroporation* or *reversible electrical breakdown* wherein the pores will eventually reseal after the electric field is removed. However, if $\Delta\Psi_m$ is much higher than the membrane dielectric constant, *irreversible electroporation* (IRE) will take place in which pores are either irreversibly enlarged or entire liposomal fragmentation occurs (Tsong, 1991). In this study we used a range of electric fields that cover both the reversible and irreversible electroporation regimes. The electric fields chosen are commonly used for *in vivo* electroporation studies and should not cause adverse cardiovascular or neurological events in animals (Jiang et al., 2015). It should be noted that for the higher electric

field strengths tested, such as 2000 $V \cdot cm^{-1}$, cell membrane dissociation and death will occur in the treatment region, but this is a desirable outcome for many applications such as tissue ablation.

We first investigated the effects of liposomal size and electric field strength on the percent release of CF from electroporated liposomes, and although they followed the relationship implied by (3), they alone were insufficient to increase the percent release of DPPC or POPC liposomes above 30%. Besides these two parameters, electroporation-induced drug release can also be modulated by adjusting the physical properties of the lipid membrane through control of the lipid composition. The main physical aspect of the membrane likely to be implicated in the response to electroporation is its fluidity. This is chiefly governed by the thermodynamic state of the bilayer: the ordered gel phase below the transition temperature, $T_m$, or the liquid crystalline phase above $T_m$. Originally, we hypothesized that liposomes in the more fluid liquid crystalline phase would be more vulnerable to electric field-induced membrane deformation compared to liposomes in the more rigid gel phase, thus leading to increased drug release (Knorr et al., 2010; Perrier et al., 2018). However, when we tested the electroporation-induced release of CF between POPC and DPPC liposomes, the gel phase DPPC liposomes exhibited a higher release than the liquid crystalline phase POPC liposomes. In fact, as argued by Weaver, there is much evidence that the biochemical composition of the membrane has a very minor impact on the $\Delta\Psi_m$, with the onset of electroporation dominated by the strength of the electric field (Weaver, 1993). Instead, membrane composition and its resulting impact on fluidity likely play a larger role *after* removal of the electric field, where membrane fluidity/rigidity impacts the speed of pore resealing. Numerous studies have shown that the time frame for pore resealing can be on the order of seconds to minutes (Glaser et al., 1988; Hibino et al., 1993; Rols and Teissié, 1990; Sukharev et al., 1992). This is much longer than the length of the electroporation pulse (here 100 μs), meaning that diffusional release of drug

in the timeframe between electric field removal and pore resealing largely exceeds the amount of drug released due to the diffusional and electrophoretic driving forces during the pulse itself. As demonstrated by Knorr et al. (Knorr et al., 2010) and Rols et al. (Rols et al., 1990), membranes with higher lipid mobility and fluidity, as in fluid-state POPC liposomes, are quicker to reseal their pores after each pulse. This would suggest less overall drug release, which is what we observed.

By selecting a DPPC parent liposome and then varying the levels of the other two components – cholesterol and BL – we were able to further increase the percent of CF released during electroporation treatment. Cholesterol displayed a biphasic effect on electroporation-induced release, with a local maximum occurring around 20% cholesterol. In gel state membranes, like DPPC liposomes at room temperature, cholesterol's rigid and bulky structure disrupts the close packing of the saturated phospholipid alkyl chains, thus promoting increased fluidity (Coderch et al., 2000; Ohvo-Rekilä et al., 2002). The increase in alkyl chain mobility presumably leads to a faster resealing of membrane pores and a concomitant decrease in the percent release of CF. Shorter pore lifetimes can also be rationalized from the knowledge that for many lipid bilayers, cholesterol increases the line tension of the pores, a driving force for pore resealing (Karatekin et al., 2003; Portet and Dimova, 2010; Zhelev and Needham, 1993). This hypothesis of decreased pore lifetime appears to be substantiated by the data for DPPC liposomes with increasing cholesterol content beyond 20%. However, small amounts of cholesterol (10 - 20%) *increase* the percent release relative to 0% or > 30% cholesterol DPPC liposomes. One possible explanation is the tendency for cholesterol to preferentially localize in gaps or defects in the packing of the lipid membrane (Bhattacharya and Haldar, 2000). This would effectively decrease membrane fluidity for small amounts of cholesterol, whereas larger amounts would begin disrupting the bulk phospholipid packing and increase fluidity. Additionally, Sułkowski et al. showed that 20%

cholesterol in DPPC liposomes promotes a favorable conformation of phospholipids by limiting the interaction of neighboring phospholipid head groups (Sułkowski et al., 2005).

Increasing the composition of BL had the surprising effect of substantially increasing the electroporation-induced release of CF from liposomes. Interestingly this effect is almost binary, with a large jump in percent release between 0% and 0.1% BL but little further change upon increasing the amount of BL up to 20%. Although little research has been done on the effects of BLs on the fluidity of membranes, Swamy et. al. determined the phase transition temperature for the BL used in this study (1,2-dipalmitoyl-sn-glycero-3-phosphoethanolamine-N-(biotinyl)) to be 40.7 ºC, which is very similar to that of DPPC (41ºC) (Swamy et al., 1994). This implies that the observed effect of BL on the percent release of CF is not mediated by changing the apparent phase transition temperature of the liposome. Rather, Swamy et al. also showed that due to the hydrophobic nature of biotin, saturated phospholipids bearing it as a headgroup tend to pack themselves in the lipid membrane in a way that interdigitates their acyl chains with those of surrounding phospholipids (Swamy et al., 1993). Chain interdigitation could lead to a decrease in phospholipid mobility, resulting in longer times for pore resealing following electroporation. This would explain the increased release of CF from liposomes containing BL. As an additional benefit, not only does increasing the percentage of BL increase the amount of cargo released during electroporation, but it also increases the probability of liposomes tethering to the streptavidin functionalized scaffold.

In addition to maximizing the release of drug during electroporation, we also wanted to minimize passive, non-induced release at physiological temperatures. Although a 60:20:20 liposome formulation was shown to provide the highest electroporation-induced drug release, it was suboptimal for physiological stability at 37 ºC due to higher levels of both cholesterol and BL.

Regarding cholesterol, several studies have indicated that it *reduces* membrane permeability in both the ordered gel and liquid crystalline states (Bhattacharya and Haldar, 2000; Hofmann et al., 2020; Kirby et al., 1980). However, in our particular system liposomes are being incubated at physiological temperature, which is just under the transition temperature for a pure DPPC liposome (41 ºC). As mentioned earlier, cholesterol is known to fluidize gel state membranes, which results in a broadening of the transition temperature below 41 ºC, much closer to 37 ºC (Eze, 1991). Thus, these liposomes are likely existing in an intermediate state between the gel and liquid crystalline states. Several studies have shown that liposome permeability is maximized in such a case, arguing that defects occurring on the gel and liquid crystalline phase boundaries allow for the facilitated escape of encapsulated molecules (Blok et al., 1975; Grit and Crommelin, 1993; Shimanouchi et al., 2009). Regarding BL, Rongen et al. linked the increase of its percent composition in DPPC liposomes to a concomitant increase in membrane permeability, although the mechanism is not well understood (Rongen et al., 1994). By reducing the levels of cholesterol and BL to 10% each, we were able to recover some liposomal stability while still maintaining the same level of electroporation-induced percent release (58 ± 7% for 80:10:10 compared to 57 ± 1% for 60:20:20).

After optimizing liposome formulation for both maximal release and increased physiological stability, we demonstrated the successful electroporation-induced release of a therapeutic protein (TNF-α) from a biomaterial scaffold. To our knowledge, this is the first example in literature of electroporation-mediated liposomal drug release from a solid phase. Such a technology stands to further expand the repertoire of multifunctional scaffold technologies for tissue engineering and assist in the development of electroporation-based therapies. For example, gene electrotransfer, the process of transfecting cells with plasmid DNA by increasing their bilayer

permeability via electroporation, has shown promise in the gene therapy field for mediating wound healing (Steinstraesser et al., 2014), DNA vaccination (Dayball et al., 2003; Escoffre et al., 2009), and erythropoietin therapy (Kreiss et al., 1999). However, it is known to be hampered by the poor mobility of injected DNA in tissues (Escoffre et al., 2009; Haberl and Pavlin, 2010) as successful transfection will only occur where the plasmid is available within the region of electroporated tissue (Chabot et al., 2019). Using an implantable scaffold with tethered DNA-encapsulating liposomes would ensure that the plasmid cargo is distributed evenly throughout the entire region of interest during electroporation. For this application, where cell death is undesirable, a lower electric field should be used, which might require further optimizing other electroporation parameters, such as the number or timing of the pulses, to achieve sufficient liposomal release.

For other applications, such as cancer treatment, localized cell death is in fact the goal, meaning higher electric fields (1500 or 2000 $V \cdot cm^{-1}$) are appropriate. For example, electrically-triggered release from scaffold-bound liposomes could be used in conjunction with electrochemotherapy, an electroporation-mediated cancer treatment that decreases the necessary dose of hydrophilic drugs like bleomycin and cisplatin by increasing their access to target cell cytosol through cell membrane permeabilization (Jaroszeski et al., 2000; Orlowski et al., 1988; Yarmush et al., 2014). Finally, it can also complement a nascent cancer treatment known as electroimmunotherapy (Geboers et al., 2020; Zhao et al., 2019), which couples the immunogenic cell death of IRE-induced tumor ablation with concurrent administration of immunostimulatory biologic drugs to induce a systemic anti-tumor immune response. Here, IRE can be used to simultaneously ablate the cancerous tissue and release a payload of immunostimulatory agents from proximally implanted scaffold-bound liposomes.

It is important to note that limitations with this system remain. Firstly, despite increasing the physiological stability of the liposomes by lowering the levels of cholesterol and BL, considerable passive leakage still occurs. To address this issue, future iterations of the liposomes could use 1,2-distearoyl-sn-glycero-3-phosphocholine (DSPC) (Anderson and Omri, 2004) instead of DPPC as the predominant lipid, which has a phase transition temperature (55 ºC) that is much higher than physiological temperatures compared to DPPC. Secondly, it will be necessary to show that scaffold-bound liposomes remain stable when exposed to serum-containing, biological media. It is possible that the higher protein concentration could destabilize the liposomes leading to premature release, which might require adjustment of the liposomal formulation (Magin and Niesman, 1984). If these limitations are addressed, liposome-coated tissue scaffolds have the potential to improve the efficacy of electroporation-based therapies.

## 5. Conclusion

Electroporation is a facile way to generate inducible drug release from liposomal carriers. This, in turn, greatly extends the utility of liposomal drug delivery, especially for time-sensitive treatments or when the cargo needs to interact with cell surface receptors for therapeutic efficacy. Here we raised the efficiency of electroporation-induced liposomal drug release. By increasing the strength of the electroporation parameters and optimizing liposomal composition, we achieved a significant increase in the percent drug release from electroporated liposomes over previously reported attempts. Additionally, we demonstrated the development of a liposome-coated PCL scaffold with the ability to release a payload of protein biologics from a localized, solid phase. Such a device could find use in the controlled tailoring of cellular microenvironments. We also showed that further optimization of the liposomal composition has the potential to increase the

thermal stability of the liposomes, thus positioning this technology as a unique and promising tool for on-demand release of bioactive molecules from tissue engineering scaffolds.

**Acknowledgments:** The authors would like to thank Prof. Joseph Zasadzinski for his helpful assistance with Cryo-SEM analysis and discussion of the effects of liposomal composition on membrane lysis. Portions of this work were carried out in the Characterization Facility, University of Minnesota, which receives partial support from the NSF through the MRSEC (Award Number DMR-2011401) and the NNCI (Award Number ECCS-2025124) programs. Specifically, the Hitachi SU8320 cryo-SEM and cryospecimen preparation system were provided by NSF MRI DMR-1229263. Other portions of this work were conducted in the Minnesota Nano Center, which is supported by the National Science Foundation through the National Nanotechnology Coordinated Infrastructure (NNCI) under Award Number ECCS-2025124.

**Author contributions**: AS: Conceptualization, Investigation, Methodology, Writing – Review and Editing; JV: Investigation, Methodology, Formal analysis, Writing – original draft, Writing – Review and Editing; FP: Conceptualization, Investigation, Methodology; MK: Methodology; QS: Writing – Review and Editing; HSL: Resources, Investigation; JB: Conceptualization; SA: Conceptualization, Funding Acquisition, Supervision, Writing – Review and Editing, Project Administration

**Declarations of interest:** None

**Funding:** This study was supported by the Dr. Ralph and Marian Falk Medical Research Trust Bank of America, N.A., NSF CBET-1845366, NIH T32GM008347 (J.V.), and the University of Minnesota's Office of Undergraduate Research (A.S.).

**References**


Altin, J.G., Parish, C.R., 2006. Liposomal vaccines-targeting the delivery of antigen. Methods 40, 39–52. https://doi.org/10.1016/j.ymeth.2006.05.027

Anderson, M., Omri, A., 2004. The Effect of Different Lipid Components on the in Vitro Stability and Release Kinetics of Liposome Formulations. Drug Deliv. 11, 33–39. https://doi.org/10.1080/10717540490265243

Anderson, P.M., Hanson, D.C., Hasz, D.E., Halet, M.R., Blazar, B.R., Ochoa, A.C., 1994. Cytokines in liposomes: Preliminary studies with IL-1, IL-2, IL-6, GM-CSF and interferon-γ. Cytokine 6, 92–101. https://doi.org/10.1016/1043-4666(94)90014-0

Azarin, S.M., Yi, J., Gower, R.M., Aguado, B.A., Sullivan, M.E., Goodman, A.G., Jiang, E.J., Rao, S.S., Ren, Y., Tucker, S.L., Backman, V., Jeruss, J.S., Shea, L.D., 2015. In vivo capture and label-free detection of early metastatic cells. Nat. Commun. 6, 1–9. https://doi.org/10.1038/ncomms9094

Belhadj, Z., Zhan, C., Ying, M., Wei, X., Xie, C., Yan, Z., Lu, W., 2017. Multifunctional targeted liposomal drug delivery for efficient glioblastoma treatment. Oncotarget 8, 66889–66900. https://doi.org/10.18632/oncotarget.17976

Bhattacharya, S., Haldar, S., 2000. Interactions between cholesterol and lipids in bilayer membranes. Role of lipid headgroup and hydrocarbon chain-backbone linkage. Biochim. Biophys. Acta - Biomembr. 1467, 39–53. https://doi.org/10.1016/S0005-2736(00)00196-6

Blok, M.C., Van Der Neut-Kok, E.C.M., Van Deenen, L.L.M., De Gier, J., 1975. The effect of chain length and lipid phase transitions on the selective permeability properties of liposomes. BBA - Biomembr. 406, 187–196. https://doi.org/10.1016/0005-2736(75)90003-6

Briuglia, M.L., Rotella, C., McFarlane, A., Lamprou, D.A., 2015. Influence of cholesterol on liposome stability and on in vitro drug release. Drug Deliv. Transl. Res. 5, 231–242. https://doi.org/10.1007/s13346-015-0220-8

Chabot, S., Bellard, E., Reynes, J.P., Tiraby, G., Teissie, J., Golzio, M., 2019. Bioelectrochemistry Electrotransfer of CpG free plasmids enhances gene expression in skin. Bioelectrochemistry 130, 1–7. https://doi.org/10.1016/j.bioelechem.2019.107343

Cheung, A.S., Zhang, D.K.Y., Koshy, S.T., Mooney, D.J., 2018. Scaffolds that mimic antigen-presenting cells enable ex vivo expansion of primary T cells. Nat. Biotechnol. 36, 160–169. https://doi.org/10.1038/nbt.4047

Chu, C., Xu, P., Zhao, H., Chen, Q., Chen, D., Hu, H., Zhao, X., Qiao, M., 2016. Effect of surface ligand density on cytotoxicity and pharmacokinetic profile of docetaxel loaded liposomes. Asian J. Pharm. Sci. 11, 655–661. https://doi.org/10.1016/j.ajps.2016.04.001

Coderch, L., Fonollosa, J., De Pera, M., Estelrich, J., De La Maza, A., Parra, J.L., 2000. Influence of cholesterol on liposome fluidity by EPR Relationship with percutaneous absorption. J. Control. Release 68, 85–95. https://doi.org/10.1016/S0168-3659(00)00240-6

Costa, A.P., Xu, X., Burgess, D.J., 2014. Freeze-anneal-thaw cycling of unilamellar liposomes: Effect on encapsulation efficiency. Pharm. Res. 31, 97–103. https://doi.org/10.1007/s11095-013-1135-z

Davalos, R. V., Mir, L.M., Rubinsky, B., 2005. Tissue ablation with irreversible electroporation. Ann. Biomed. Eng. 33, 223–231. https://doi.org/10.1007/s10439-005-8981-8

Dayball, K., Millar, J., Miller, M., Wan, Y.H., Bramson, J., 2003. Electroporation Enables Plasmid Vaccines to Elicit CD8 + T Cell Responses in the Absence of CD4 + T Cells. J. Immunol. 171, 3379–3384. https://doi.org/10.4049/jimmunol.171.7.3379

Denzi, A., della Valle, E., Francesca, A., Marie, B., Mir, L.M., Liberti, M., 2017. Exploring the Applicability of Nano-Poration for Remote Control in Smart Drug Delivery Systems. J. Membr. Biol. 250, 31–40. https://doi.org/10.1007/s00232-016-9922-1

Escoffre, J., Mauroy, C., Portet, T., Wasungu, L., Paganin-Gioanni, A., Golzio, M., Teissie, J., Rols, M., 2009. Gene electrotransfer : from biophysical mechanisms to in vivo applications. Biophys Rev 1, 185–191. https://doi.org/10.1007/s12551-009-0019-2

Eze, M.O., 1991. Phase Transitions in Phospholipid Bilayers: Lateral Phase Separations Play Vital Roles in Biomembranes. Biochem. Educ. 19, 204–208. https://doi.org/10.1016/0307-4412(91)90103-F

Feiner, R., Fleischer, S., Shapira, A., Kalish, O., Dvir, T., 2018. Multifunctional degradable electronic scaffolds for cardiac tissue engineering. J. Control. Release 281, 189–195. https://doi.org/10.1016/j.jconrel.2018.05.023

Forbes, N., Pallaoro, A., Reich, N.O., Zasadzinski, J.A., 2014. Rapid, Reversible Release from Thermosensitive Liposomes Triggered by Near-Infra-Red Light. Part. Part. Syst. Charact. 31, 1158–1167. https://doi.org/10.1002/ppsc.201400035

Gabizon, A., Papahadjopoulos, D., 1988. Liposome formulations with prolonged circulation time in blood and enhanced uptake by tumors. Proc. Natl. Acad. Sci. U. S. A. 85, 6949–6953. https://doi.org/10.1073/pnas.85.18.6949

Geboers, B., Scheffer, H.J., Graybill, P.M., Ruarus, A.H., Nieuwenhuizen, S., Puijk, R.S., van den Tol, P.M., Davalos, R. V, Rubinsky, B., de Gruijl, T.D., Miklavčič, D., Meijerink, M.R., 2020. High-Voltage Electrical Pulses in Oncology : Irreversible Electroporation, Electrochemotherapy, Gene Electrotransfer, Electrofusion, and Electroimmunotherapy. Radiology 295, 254–272. https://doi.org/10.1148/radiol.2020192190

Glaser, R.W., Leikin, S.L., Chernomordik, L. V., Pastuchenko, V.F., Sokirko, A.I., 1988. Reversible electrical breakdown of lipid bilayers: formation and evolution of pores. Biochim. Biophys. Acta 940, 275–287. https://doi.org/10.1016/0005-2736(88)90202-7

Golberg, A., Yarmush, M.L., 2013. Nonthermal irreversible electroporation: Fundamentals, applications, and challenges. IEEE Trans. Biomed. Eng. 60, 707–714. https://doi.org/10.1109/TBME.2013.2238672

Grit, M., Crommelin, D.J.A., 1993. Chemical stability of liposomes: implications for their physical stability. Chem. Phys. Lipids 64, 3–18. https://doi.org/10.1016/0009-3084(93)90053-6

Guo, Z., Jiang, N., Moore, J., Mccoy, C.P., Ziminska, M., Ra, C., Sarri, G., Hamilton, A.R., Li, Y., Zhang, L., Zhu, S., Sun, D., 2019. Nanoscale Hybrid Coating Enables Multifunctional Tissue Scaffold for Potential Multimodal Therapeutic Applications. ACS Appl. Mater. Interfaces 11, 27269−27278. https://doi.org/10.1021/acsami.9b04278

Haberl, S., Pavlin, M., 2010. Use of Collagen Gel as a Three-Dimensional In Vitro Model to Study Electropermeabilization and Gene Electrotransfer. J. Membr. Biol. 236, 87–95. https://doi.org/10.1007/s00232-010-9280-3

Hibino, M., Itoh, H., Kinosita, K., 1993. Time courses of cell electroporation as revealed by submicrosecond imaging of transmembrane potential. Biophys. J. 64, 1789–1800. https://doi.org/10.1016/S0006-3495(93)81550-9

Hofmann, C., Kaiser, B., Maerkl, S., Duerkop, A., Baeumner, A.J., 2020. Cationic liposomes for generic signal amplification strategies in bioassays. Anal. Bioanal. Chem. 412, 3383–3393. https://doi.org/10.1007/s00216-020-02612-w

Jaroszeski, M.J., Dang, V., Pottinger, C., Hickey, J., Gilbert, R., Heller, R., 2000. Toxicity of

anticancer agents mediated by electroporation in vitro. Anticancer. Drugs 11, 201–208. https://doi.org/10.1097/00001813-200003000-00008
Jiang, C., Davalos, R. V., Bischof, J.C., 2015. A review of basic to clinical studies of irreversible electroporation therapy. IEEE Trans. Biomed. Eng. 62, 4–20. https://doi.org/10.1109/TBME.2014.2367543
Karal, M.A.S., Ahamed, M.K., Mokta, N.A., Ahmed, M., Ahammed, S., 2020. Influence of cholesterol on electroporation in lipid membranes of giant vesicles. Eur. Biophys. J. 49, 361–370. https://doi.org/10.1007/s00249-020-01443-y
Karatekin, E., Sandre, O., Guitouni, H., Borghi, N., Puech, P.H., Brochard-Wyart, F., 2003. Cascades of transient pores in giant vesicles: Line tension and transport. Biophys. J. 84, 1734–1749. https://doi.org/10.1016/S0006-3495(03)74981-9
Kedar, E., Palgi, O., Golod, G., Babai, I., Barenholz, Y., 1997. Delivery of Cytokines by Liposomes. III. Liposome-Encapsulated GM-CSF and TNF-alpha Show Improved Pharmacokinetics and Biological Activity and Reduced Toxicity in Mice. J. Immunother. 20, 180–193. https://doi.org/10.1097/00002371-199705000-00003
Kim, D.W., Andres, M.L., Miller, G.M., Cao, J.D., Green, L.M., Seynhaeve, A.L.B., Ten Hagen, T.L.M., Gridley, D.S., 2002. Immunohistological analysis of immune cell infiltration of a human colon tumor xenograft after treatment with Stealth liposome-encapsulated tumor necrosis factor-alpha and radiation. Int. J. Oncol. 21, 973–979. https://doi.org/10.3892/ijo.21.5.973
Kirby, C., Clarke, J., Gregoriadis, G., 1980. Effect of the cholesterol content of small unilamellar liposomes on their stability in vivo and in vitro. Biochem. J. 186, 591–598. https://doi.org/10.1042/bj1860591
Knorr, R.L., Staykova, M., Gracià, R.S., Dimova, R., 2010. Wrinkling and electroporation of giant vesicles in the gel phase. Soft Matter 6, 1990–1996. https://doi.org/10.1039/b925929e
Kotnik, T., Kramar, P., Pucihar, G., Miklavčič, D., Tarek, M., 2012. Cell membrane electroporation - Part 1: The phenomenon. IEEE Electr. Insul. Mag. 28, 14–23. https://doi.org/10.1109/MEI.2012.6268438
Kreiss, P., Bettan, M., Crouzet, J., Scherman, D., 1999. Erythropoietin Secretion and Physiological Effect in Mouse after Intramuscular Plasmid DNA Electrotransfer. J. Gene Med. 1, 245–250. https://doi.org/10.1002/(SICI)1521-2254(199907/08)1:4<245::AID-JGM49>3.0.CO;2-G
Kulbacka, J., Pucek, A., Kotulska, M., Dubinska-Magiera, M., Rossowska, J., Rols, M.-P., Wilk, K.A., 2016. Electroporation and lipid nanoparticles with cyanine IR-780 and flavonoids as efficient vectors to enhanced drug delivery in colon cancer. Bioelectrochemistry 110, 19–31. https://doi.org/10.1016/j.bioelechem.2016.02.013
Lam, T., Moy, A., Lee, H.R., Shao, Q., Bischof, J.C., Azarin, S.M., 2020. Iron oxide-loaded polymer scaffolds for non-invasive hyperthermic treatment of infiltrated cells. AIChE J. 66, e17001. https://doi.org/10.1002/aic.17001
Lamichhane, T.N., Raiker, R.S., Jay, S.M., 2015. Exogenous DNA Loading into Extracellular Vesicles via Electroporation is Size-Dependent and Enables Limited Gene Delivery. Mol. Pharm. 12, 3650–3657. https://doi.org/10.1021/acs.molpharmaceut.5b00364
Machy, P., Lewis, F., McMillan, L., Jonak, Z.L., 1988. Gene transfer from targeted liposomes to specific lymphoid cells by electroporation. Proc. Natl. Acad. Sci. U. S. A. 85, 8027–8031. https://doi.org/10.1073/pnas.85.21.8027
Magin, R.L., Niesman, M.R., 1984. Temperature-dependent permeability of large unilamellar

liposomes. Chem. Phys. Lipids 34, 245–256. https://doi.org/10.1016/0009-3084(84)90059-8
Mbawuike, I.N., Wyde, P.R., Anderson, P.M., 1990. Enhancement of the protective efficacy of inactivated influenza A virus vaccine in aged mice by IL-2 liposomes. Vaccine 8, 347–352. https://doi.org/10.1016/0264-410X(90)90093-2
Mulligan, M.J., Lyke, K.E., Kitchin, N., Absalon, J., Gurtman, A., Lockhart, S., Neuzil, K., Raabe, V., Bailey, R., Swanson, K.A., Li, P., Koury, K., Kalina, W., Cooper, D., Fontes-Garfias, C., Shi, P., Türeci, Ö., Tompkins, K.R., Walsh, E.E., Frenck, R., Falsey, A.R., Dormitzer, P.R., Gruber, W.C., Şahin, U., Jansen, K.U., 2020. Phase I / II study of COVID-19 RNA vaccine BNT162b1 in adults. Nature 586, 589–593. https://doi.org/10.1038/s41586-020-2639-4
Nisbet, D.R., Yu, L.M.Y., Zahir, T., Forsythe, J.S., Shoichet, M.S., 2008. Characterization of neural stem cells on electrospun poly(ε-caprolactone) submicron scaffolds: evaluating their potential in neural tissue engineering. J. Biomater. Sci. Polym. Ed. 19, 623–634. https://doi.org/10.1163/156856208784089652
Niu, M., Lu, Y., Hovgaard, L., Wu, W., 2011. Liposomes containing glycocholate as potential oral insulin delivery systems: preparation, in vitro characterization, and improved protection against enzymatic degradation. Int. J. Nanomedicine 6, 1155–1166. https://doi.org/10.2147/ijn.s19917
Ohvo-Rekilä, H., Ramstedt, B., Leppimäki, P., Slotte, J.P., 2002. Cholesterol interactions with phospholipids in membranes. Prog. Lipid Res. 41, 66–97. https://doi.org/10.1016/S0163-7827(01)00020-0
Orlowski, S., Belehradek Jr., J., Paoletti, C., Mir, L.M., 1988. Transient Electropermeabilization of Cells in Culture - Increase of the Cytotoxicity of Anticancer Drugs. Biochem. Pharmacol. 37, 4727–4733. https://doi.org/10.1016/0006-2952(88)90344-9
Pelaez, F., Manuchehrabadi, N., Roy, P., Natesan, H., Wang, Y., Racila, E., Fong, H., Zeng, K., Silbaugh, A.M., Bischof, J.C., Azarin, S.M., 2018. Biomaterial scaffolds for non-invasive focal hyperthermia as a potential tool to ablate metastatic cancer cells. Biomaterials 166, 27–37. https://doi.org/10.1016/j.biomaterials.2018.02.048
Pelaez, F., Shao, Q., Ranjbartehrani, P., Lam, T., Lee, H.R., O'Flanagan, S., Silbaugh, A., Bischof, J.C., Azarin, S.M., 2020. Optimizing Integrated Electrode Design for Irreversible Electroporation of Implanted Polymer Scaffolds. Ann. Biomed. Eng. 48, 1230–1240. https://doi.org/10.1007/s10439-019-02445-4
Perrier, D.L., Rems, L., Kreutzer, M.T., Boukany, P.E., 2018. The role of gel-phase domains in electroporation of vesicles. Sci. Rep. 8, 4758. https://doi.org/10.1038/s41598-018-23097-9
Pomatto, M., Bussolati, B., D'Antico, S., Ghiotto, S., Tetta, C., Brizzi, M.F., Camussi, G., 2019. Improved Loading of Plasma-Derived Extracellular Vesicles to Encapsulate Antitumor miRNAs. Mol. Ther. Methods Clin. Dev. 13, 133–144. https://doi.org/10.1016/j.omtm.2019.01.001
Portet, T., Dimova, R., 2010. A new method for measuring edge tensions and stability of lipid bilayers: Effect of membrane composition. Biophys. J. 99, 3264–3273. https://doi.org/10.1016/j.bpj.2010.09.032
Rao, S.S., Bushnell, G.G., Azarin, S.M., Spicer, G., Aguado, B.A., Stoehr, J.R., Jiang, E.J., Backman, V., Shea, L.D., Jeruss, J.S., 2016. Enhanced survival with implantable scaffolds that capture metastatic breast cancer cells in vivo. Cancer Res. 76, 5209–5218. https://doi.org/10.1158/0008-5472.CAN-15-2106
Retelj, L., Pucihar, G., Miklavcic, D., 2013. Electroporation of Intracellular Liposomes Using

Nanosecond Electric Pulses — A Theoretical Study. IEEE Trans. Biomed. Eng. 60, 2624–2635. https://doi.org/10.1109/TBME.2013.2262177
Rols, M.P., Dahhou, F., Mishra, K.P., Teissie, J., 1990. Control of Electric Field Induced Cell Membrane Permeabilization by Membrane Order. Biochemistry 29, 2960–2966. https://doi.org/10.1021/bi00464a011
Rols, M.P., Teissié, J., 1990. Electropermeabilization of mammalian cells. Quantitative analysis of the phenomenon. Biophys. J. 58, 1089–1098. https://doi.org/10.1016/S0006-3495(90)82451-6
Rongen, H.A.H., van der Horst, H.M., Hugenholtz, G.W.K., Bult, A., van Bennekom, W.P., van der Meide, P.H., 1994. Development of a liposome immunosorbent assay for human interferon-γ. Anal. Chim. Acta 287, 191–199. https://doi.org/10.1016/0003-2670(93)E0592-U
Shimanouchi, T., Ishii, H., Yoshimoto, N., Umakoshi, H., Kuboi, R., 2009. Calcein permeation across phosphatidylcholine bilayer membrane: Effects of membrane fluidity, liposome size, and immobilization. Colloids Surfaces B Biointerfaces 73, 156–160. https://doi.org/10.1016/j.colsurfb.2009.05.014
Srimathveeravalli, G., Abdel-atti, D., Perez-Medina, C., Takaki, H., Solomon, S.B., Mulder, W.J.M., Reiner, T., 2018. Reversible Electroporation – Mediated Liposomal Doxorubicin Delivery to Tumors Can Be Monitored With 89 Zr-Labeled Reporter Nanoparticles. Mol. Imaging 17, 1–9. https://doi.org/10.1177/1536012117749726
Steinstraesser, L., Lam, M.C., Jacobsen, F., Porporato, P.E., Chereddy, K.K., Becerikli, M., Stricker, I., Hancock, R.E.W., Lehnhardt, M., Sonveaux, P., Préat, V., Vandermeulen, G., 2014. Skin Electroporation of a Plasmid Encoding hCAP-18 / LL-37 Host Defense Peptide Promotes Wound Healing. Mol. Ther. 22, 734–742. https://doi.org/10.1038/mt.2013.258
Stoicheva, N.G., Hui, S.W., 1994. Electrofusion of cell-size liposomes. Biochim. Biophys. Acta 1195, 31–38. https://doi.org/https://doi.org/10.1016/0005-2736(94)90005-1
Stromberg, A., Karlsson, A., Ryttse, F., Davidson, M., Chiu, D.T., Orwar, O., 2001. Microfluidic Device for Combinatorial Fusion of Liposomes and Cells. Anal. Chem. 73, 126–130. https://doi.org/10.1021/ac000528m
Sukharev, S.I., Klenchin, V.A., Serov, S.M., Chernomordik, L. V, Chizmadzhev, Y.A., 1992. Electroporation and electrophoretic DNA transfer into cells - The effect of DNA interaction with electropores. Biophys. J. 63, 1320–1327. https://doi.org/10.1016/S0006-3495(92)81709-5
Sułkowski, W.W., Pentak, D., Nowak, K., Sułkowska, A., 2005. The influence of temperature, cholesterol content and pH on liposome stability. J. Mol. Struct. 744–747, 737–747. https://doi.org/10.1016/j.molstruc.2004.11.075
Swamy, M.J., Angerstein, B., Marsh, D., 1994. Differential scanning calorimetry of thermotropic phase transitions in vitaminylated lipids: aqueous dispersions of N-biotinyl phosphatidylethanolamines. Biophys. J. 66, 31–39. https://doi.org/10.1016/S0006-3495(94)80761-1
Swamy, M.J., Marsh, D., Würz, U., 1993. Structure of Vitaminylated Lipids in Aqueous Dispersion: X-ray Diffraction and 31P NMR Studies of N-Biotinylphosphatidylethanolamines. Biochemistry 32, 9960–9967. https://doi.org/10.1021/bi00089a011
Teissie, J., Tsong, T.Y., 1981. Electric Field Induced Transient Pores in Phospholipid Bilayer Vesicles. Biochemistry 20, 1548–1554. https://doi.org/10.1021/bi00509a022

Tsong, T.Y., 1991. Electroporation of cell membranes. Biophys. J. 60, 297–306. https://doi.org/10.1016/S0006-3495(91)82054-9
van der Veen, Alexander H., Eggermont, A.M.M., Seynhaeve, A.L.B., van Tiel, S.T., ten Hagen, T.L.M., 1998. Biodistribution and tumor localization of stealth liposomal tumor necrosis factor-α in soft tissue sarcoma bearing rats. Int. J. Cancer 77, 901–906. https://doi.org/10.1002/(SICI)1097-0215(19980911)77:6<901::AID-IJC17>3.0.CO;2-3
van der Veen, Alexander H, Eggermont, A.M.M., ten Hagen, T.L.M., 1998. Stealth® liposomal tumor necrosis factor-α in solid tumor treatment. Int. J. Pharm. 162, 87–94. https://doi.org/10.1016/s0378-5173(97)00416-x
Wassef, N.M., Alving, C.R., Richards, R.L., 1994. Liposomes as Carriers for Vaccines. Immunomethods 4, 217–222. https://doi.org/10.1006/immu.1994.1023
Weaver, J.C., 1993. Electroporation: A general phenomenon for manipulating cells and tissues. J. Cell. Biochem. 51, 426–435. https://doi.org/10.1002/jcb.2400510407
Yarmush, M.L., Golberg, A., Sersa, G., Kotnik, T., Miklavcic, D., 2014. Electroporation-Based Technologies for Medicine: Principles, Applications, and Challenges. Annu. Rev. Biomed. Eng. 16, 295–320. https://doi.org/10.1146/annurev-bioeng-071813-104622
Yi, J., Barrow, A.J., Yu, N., O'Neill, B.E., 2013. Efficient electroporation of liposomes doped with pore stabilizing nisin. J. Liposome Res. 23, 197–202. https://doi.org/10.3109/08982104.2013.788024
Yoshizaki, Y., Yuba, E., Sakaguchi, N., Koiwai, K., Harada, A., Kono, K., 2014. Potentiation of pH-sensitive polymer-modified liposomes with cationic lipid inclusion as antigen delivery carriers for cancer immunotherapy. Biomaterials 35, 8186–8196. https://doi.org/10.1016/j.biomaterials.2014.05.077
Yuyama, Y., Tsujimoto, M., Fujimoto, Y., Oku, N., 2000. Potential usage of thermosensitive liposomes for site-specific delivery of cytokines. Cancer Lett. 155, 71–77. https://doi.org/10.1016/S0304-3835(00)00410-9
Zhang, X., Qi, J., Lu, Y., He, W., Li, X., Wu, W., 2014. Biotinylated liposomes as potential carriers for the oral delivery of insulin. Nanomedicine Nanotechnology, Biol. Med. 10, 167–176. https://doi.org/10.1016/j.nano.2013.07.011
Zhao, J., Wen, Xiaofei, Tian, L., Li, T., Xu, C., Wen, Xiaoxia, Melancon, M.P., Gupta, S., Shen, B., Peng, W., Li, C., 2019. Irreversible electroporation reverses resistance to immune checkpoint blockade in pancreatic cancer. Nat. Commun. 10, 1–14. https://doi.org/10.1038/s41467-019-08782-1
Zhelev, D. V., Needham, D., 1993. Tension-stabilized pores in giant vesicles: determination of pore size and pore line tension. BBA - Biomembr. 1147, 89–104. https://doi.org/10.1016/0005-2736(93)90319-U